

# Band-Gap Modulation in Single-Crystalline $\text{Si}_{1-x}\text{Ge}_x$ Nanowires

Jee-Eun Yang, Chang-Beom Jin, Cheol-Joo Kim, and Moon-Ho Jo\*

Department of Materials Science and Engineering, Pohang University of Science and Technology (POSTECH), San 31, Hyoja-Dong, Nam-Gu, Pohang, Gyungbuk, Korea 790-784

Received June 27, 2006; Revised Manuscript Received September 27, 2006

## ABSTRACT

We report the energy band-gap modulation of single-crystalline  $\text{Si}_{1-x}\text{Ge}_x$  ( $0 \leq x \leq 1$ ) nanowires ranging from near-infrared (NIR) to visible regions by optical band-edge absorption. Single-crystalline  $\text{Si}_{1-x}\text{Ge}_x$  nanowires were grown by an Au catalyst-assisted chemical vapor synthesis using  $\text{SiH}_4$  and  $\text{GeH}_4$  precursors, and the relative composition of Si and Ge was reproducibly directed in the whole range of  $0 \leq x \leq 1$  by controlling the kinetics of catalytic decomposition of precursors near the eutectic temperature with Au. We show that, by the appropriate alloying of Si and Ge to form random solid solutions at the nanometer scale, the energy band-gap of  $\text{Si}_{1-x}\text{Ge}_x$  is tuned from 0.68 to 2.25 eV. Specifically, we demonstrate that with respect to the fundamental energy band-gap of bulk Si, the optical-absorption band edge shifts to a lower energy with increasing Ge content, and also that the band edge shifts to a higher energy with decreasing diameter of the nanowires below certain sizes. Our finding demonstrates that the energy band-gap of  $\text{Si}_{1-x}\text{Ge}_x$  nanowires can be modulated in a wider energy range and suggests implications for group-IV semiconductor nanowire photonics.

Si and Ge form a continuous series of substitutional solid solutions,  $\text{Si}_{1-x}\text{Ge}_x$  with a fixed crystal structure over the entire compositional range of  $0 \leq x \leq 1$ . These group-IV semiconductor alloys offer a continuously variable system with a wide range of crystal lattices and energy band-gaps, leading to various electrical and optical properties.<sup>1</sup> Indeed, in microelectronics,  $\text{Si}_{1-x}\text{Ge}_x$  thin films offer a lattice-engineered platform for strained Si carrier channels with enhanced carrier mobility in Si/ $\text{Si}_{1-x}\text{Ge}_x$  heterostructures.<sup>2,3</sup> More interestingly, the continuous variation in the energy-band gap in  $\text{Si}_{1-x}\text{Ge}_x$  provides challenging opportunities for Si optoelectronics because it potentially allows emission and detection of the photons in the wavelength range of optical fiber communication.<sup>4,5</sup> Light emission from these group-IV semiconductors is, however, only poorly achieved because of the relatively slow radiative recombination of electron–hole (e–h) pairs across the indirect energy band-gap.<sup>6</sup> One promising strategy to enhance luminescence efficiency, at least in Si photonics, is to spatially confine e–h pairs at the nanometer scale, that is light emission from Si nanocrystals.<sup>7,8</sup> Hence, one can speculate that efficient light emission for optical communication can be achieved from  $\text{Si}_{1-x}\text{Ge}_x$  nanocrystals whose size is smaller than their characteristic length scale for light-emission processes.<sup>9</sup> Here we report the growth of single-crystalline  $\text{Si}_{1-x}\text{Ge}_x$  nanowires, whose relative composition is controllably tuned over the entire composition range. We then present experimental demonstra-

tion of the optical band-edge shift from near-infrared to visible regions with alloying of Si and Ge, and their spatial confinement at the nanometer scale, and we interpret our observations as energy band-gap modulation in  $\text{Si}_{1-x}\text{Ge}_x$  nanowires. Specifically, we show that the optical band-edge of *thick*  $\text{Si}_{1-x}\text{Ge}_x$  nanowires can be adjusted by the *intrinsic* bulk alloying effects, and can be tuned further with the control of the diameters of the *thin*  $\text{Si}_{1-x}\text{Ge}_x$  nanowires by the *extrinsic* size effects. We note that previous reports demonstrated the growth of single-crystalline  $\text{Si}_{1-x}\text{Ge}_x$  nanowires by various catalyst-assisted syntheses, such as laser ablations, vapor transports, and chemical vapor syntheses.<sup>10–12</sup> Nevertheless, no report on the modulation of the band gaps in  $\text{Si}_{1-x}\text{Ge}_x$  nanowires, which is our primary concern of this Letter, is available to the best of our knowledge to date.

Single-crystalline  $\text{Si}_{1-x}\text{Ge}_x$  nanowires were synthesized by the Au catalyst-assisted chemical vapor process. Au catalysts of the nanometer scale were prepared by deposition of very thin Au films or colloidal Au nanoparticles on  $\text{SiO}_2/\text{Si}$  (100) or quartz substrates, and are subsequently loaded in a quartz tube furnace. Then the crystal growth was carried out under a constant flow of independent  $\text{SiH}_4$  and  $\text{GeH}_4$  precursors (specifically, 10% of  $\text{SiH}_4$  and  $\text{GeH}_4$  premixed in  $\text{H}_2$ ) at given temperatures. The resultant  $\text{Si}_{1-x}\text{Ge}_x$  nanowires were characterized by scanning electron microscopy for their morphology, and by transmission electron microscopy (TEM) and X-ray diffraction (XRD) for their crystallinity and chemical composition. The fundamental energy band-gap was esti-

\* Corresponding author. E-mail: mhjo@postech.ac.kr.

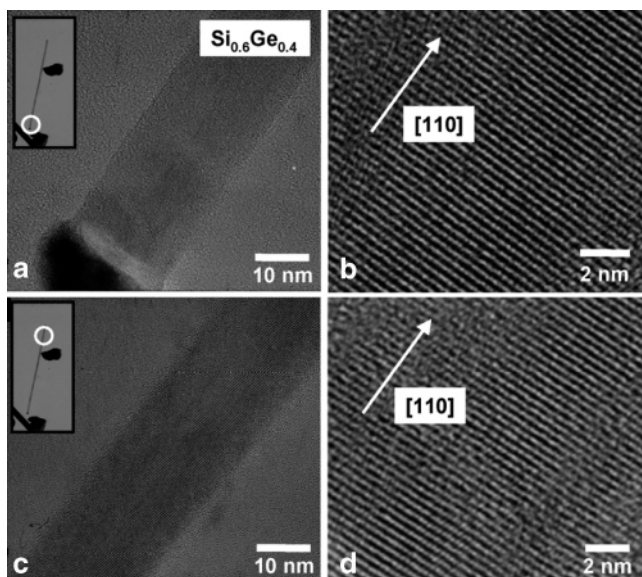


**Figure 1.** Transmission electron microscope images of an individual  $\text{Si}_{0.6}\text{Ge}_{0.4}$  nanowire. Parts a and c are the images of different locations marked with circles in the insets, and b and d are high-resolution images from the middle sections in a and c, showing that the crystal orientation along the length is [110].

mated from optical band-edge absorption measurements done on the dispersed nanowires in  $\text{D}_2\text{O}$  with appropriate concentrations or the nanowires grown on quartz substrates at room temperature.

Table 1 summarizes the growth conditions for various  $\text{Si}_{1-x}\text{Ge}_x$  nanowires of the representative compositions in this study. We have optimized the growth conditions, such as the growth temperature of 350–390 °C and the total gas pressure of 200 Torr for single-crystalline nanowires. Typically, we observed the conical shapes of  $\text{Si}_{1-x}\text{Ge}_x$  nanowires

**Table 1.** Growth conditions of  $\text{Si}_{1-x}\text{Ge}_x$  nanowires for various compositions in this study

temperature (°C)	pressure (Torr)	gas flow rate (sccm)			Si:Ge (%)
		$\text{SiH}_4$	$\text{GeH}_4$	$\text{H}_2$	
370–390	200	80	3	45	65:35
370–390	200	50	5	45	45:55
370–390	200	50	10	45	35:65
350–390	200	50	20	45	30:70
350–390	200	30	30	45	20:80
350–390	200	10	50	45	15:85

at above 400 °C, particularly for the Ge-rich nanowires, and found that the introduction of  $\text{H}_2$  gas during the growth effectively suppressed the formation of conical shape at given temperatures.<sup>13,14</sup> To modulate the relative composition of Si and Ge in the  $\text{Si}_{1-x}\text{Ge}_x$  nanowires, we systematically vary the precursor gas-flow rates of  $\text{SiH}_4$  and  $\text{GeH}_4$  in the total pressure of 200 Torr. Figure 1 shows representative TEM images of an individual  $\text{Si}_{1-x}\text{Ge}_x$  nanowire, and we observed essentially the same images as Figure 1 from other nanowires of different compositions. The observation of Au catalysts at the front tip of the nanowires, as in Figure 1a, suggests that nanowire growth is governed by the vapor–liquid–solid mechanism.<sup>15,16</sup> It is also demonstrated that the nanowires are single-crystalline with the same crystal orientation along the entire nanowire length. For example, the nanowires in Figure 1 grow in the [110] direction along the entire length direction, although it is found that the crystal orientation along the growth direction varies for the nanowires of different diameters.<sup>17</sup>

The relative composition of  $\text{Si}_{1-x}\text{Ge}_x$  nanowires is determined from energy-dispersive X-ray (EDX) spectra probed on individual nanowires by the convergent electron beam in TEM. We quantitatively determined the relative composition

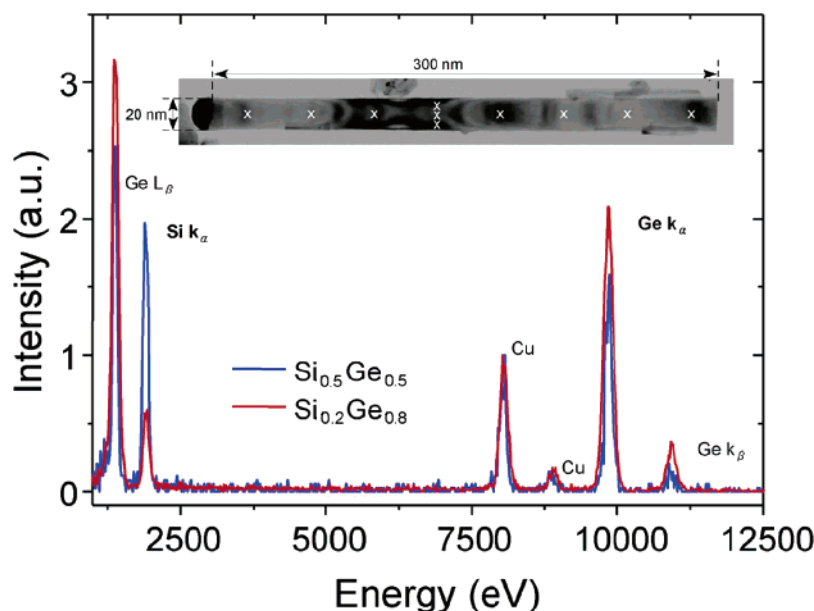


**Figure 2.** Energy-dispersive X-ray (EDX) spectra collected from individual  $\text{Si}_{0.2}\text{Ge}_{0.8}$  and  $\text{Si}_{0.5}\text{Ge}_{0.5}$  nanowires. The relative composition of Si and Ge is determined using the  $k$  factor of Si and Ge  $\text{K}\alpha$  radiation in the spectra. The inset is a TEM image of a  $\text{Si}_{0.5}\text{Ge}_{0.5}$  nanowire, and the EDX spectra were collected from different positions within the nanowires as marked with x, and showed essentially the same compositions within 5% variation.

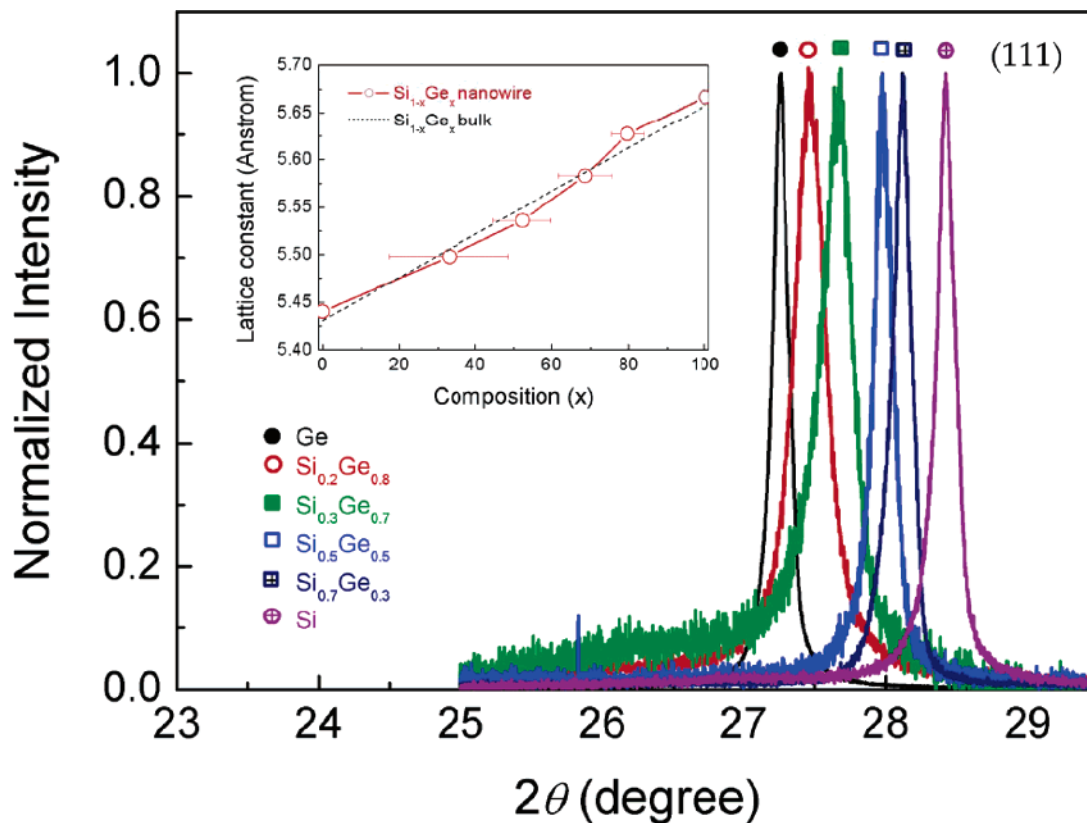


**Figure 3.** X-ray diffraction  $\theta$ – $2\theta$  scans of  $\text{Si}_{1-x}\text{Ge}_x$  nanowires of six representative compositions,  $0 \leq x \leq 1$ . The peaks are (111) diffractions of the diamond structure and progressively shift between those of Si and Ge nanowires. Arrays of nanowires in the XRD measurements showed the mean diameter of 20 nm. The full width at half-maximum in each peak is  $0.14^\circ$ ,  $0.258^\circ$ ,  $0.258^\circ$ ,  $0.158^\circ$ ,  $0.152^\circ$ , and  $0.156^\circ$ , respectively, as Ge content decreases. The inset shows the variation in lattice constants as a function of composition, extracted from the (111) diffractions.

using the  $k$  factor of Si and Ge  $K\alpha$  radiation in the EDX spectra, as representatively shown for  $\text{Si}_{0.5}\text{Ge}_{0.5}$  and  $\text{Si}_{0.2}\text{Ge}_{0.8}$  nanowires in Figure 2. We found for each nanowire that the composition is almost invariant within 5% variation in both radial and axial directions of the nanowire, see the inset. We have not found any evidence of phase inhomogeneity within the limit of our characterizations, that is, no obvious Ge segregation within the nanowires, as often found in thin-film chemical vapor depositions.<sup>18</sup> This finding confirms appropriate alloying of Si and Ge to form random substitutional alloy nanowires. We note that there is a finite diameter distribution in a batch of the nanowire samples due to the size variation of the Au catalysts, and interestingly we found the systematic variation by small amounts in the composition of  $\text{Si}_{1-x}\text{Ge}_x$  nanowires for different diameters. For example, there is slightly higher Ge content in the thicker  $\text{Si}_{1-x}\text{Ge}_x$  nanowires within a sample batch, and this is presumably due to different kinetics of the thermal decompositions of the precursors on catalysts of different sizes. The composition of each batch of the nanowire samples was then represented from the EDX spectra collected from the nanowires of the mean diameter in the batch of each growth condition. Nevertheless, we stress here that the qualitative conclusions that we present in this study, such as modulation of lattice constants and energy band-gaps with alloying and mean-diameter control that were measured on random arrays of

nanowires, are not affected regardless of this statistical variation in diameters within a sample batch.

Lattice constants of  $\text{Si}_{1-x}\text{Ge}_x$  nanowires are determined from the (111) diffraction of the diamond structure in the  $\theta$ – $2\theta$  XRD scan done on an array of nanowires whose mean diameter is 20 nm, as shown in Figure 3. It shows that with increasing Ge content the (111) diffraction peak in  $\text{Si}_{1-x}\text{Ge}_x$  nanowires progressively shifts to lower angles from that of Si nanowires to that of Ge nanowires. The variation in lattice constant is summarized in the inset, and it roughly follows the general trend of bulk  $\text{Si}_{1-x}\text{Ge}_x$  in Vegard limit.<sup>19</sup> The other XRD peaks such as (220) and (311) diffractions (not shown) exhibit the same trends as a function of composition for the variation in lattice constants. This finding also confirms appropriate alloying of Si and Ge in our  $\text{Si}_{1-x}\text{Ge}_x$  nanowires. It is notable that the full width at the half-maximum of the diffraction peaks in alloy nanowires is wider than those of parent elemental nanowires, see the Figure caption. We attribute this to the slight variation of the composition due to the diameter distribution in the XRD samples, as discussed above.

The optical absorption spectra of  $\text{Si}_{1-x}\text{Ge}_x$  nanowires were collected in the energy ranges of the fundamental energy band-gaps of bulk Si and Ge crystals at room temperature as in Figure 4a. To separate alloying effects in the bulk limit on optical band-edge absorption from possible size-effects,

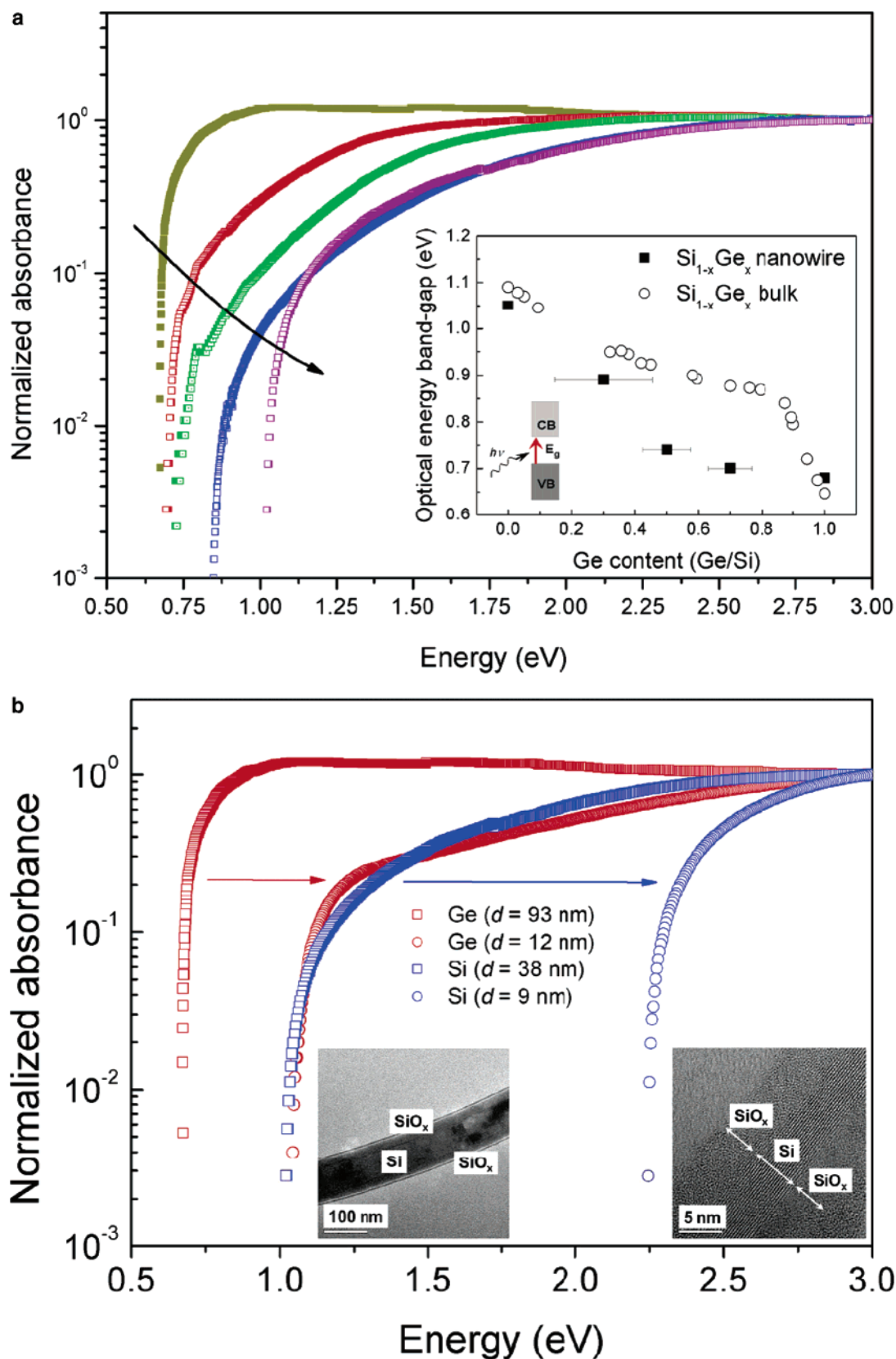


**Figure 4.** (a) Optical absorption spectra of  $\text{Si}_{1-x}\text{Ge}_x$  nanowires of five representative compositions,  $0 \leq x \leq 1$  at 300 K near the energy band-gaps. Following the arrow, the spectrum corresponds to Ge,  $\text{Si}_{0.3}\text{Ge}_{0.7}$ ,  $\text{Si}_{0.5}\text{Ge}_{0.5}$ ,  $\text{Si}_{0.7}\text{Ge}_{0.3}$ , and Si nanowires, respectively. The absorbance is normalized with the values at 3 eV in each sample for qualitative comparison. Strong absorbance due to  $\text{D}_2\text{O}$  below 0.5 eV is eliminated for clarity. The inset summarizes variation of optical band-edges from the main panel along with the known values from bulk  $\text{Si}_{1-x}\text{Ge}_x$  crystals. The mean diameters of arrays of nanowires for the measurement are greater than 40 nm. (b) Optical absorption spectra of Si and Ge nanowires with different diameters at 300 K. As the diameters of nanowires decreased to a certain size, the optical band-edges shift to higher energy by significant amounts, indicating the size effect in the absorption processes.



we have first intentionally grown  $\text{Si}_{1-x}\text{Ge}_x$  nanowires whose mean-diameters are to be greater than 40 nm and oxidized grown nanowires in  $\text{O}_2$  at 800 °C for 1 h. The spectra from different samples exhibit various intensities in optical absorbance within the same order of magnitude, primarily due to different concentration of nanowires. We identify the common features by comparing the normalized absorbance of various  $\text{Si}_{1-x}\text{Ge}_x$  nanowires in which they commonly show that with increasing energy the absorption intensity increases sharply at the certain threshold energy followed by gradual increase at higher energies up to 3.0 eV. The tendency of the gradual increase of absorbance above the threshold energy is more pronounced as Si content increases, and this trend is qualitatively consistent with optical absorption of bulk Si and Ge crystals in the literature.<sup>20,21</sup> More importantly, we attribute the onsets of absorption intensity at the threshold energy to the interband optical transitions across the edges of the energy band-gaps, as indicated in the inset. Indeed, we observed the optical band-edges of 0.68 and 1.05 eV for Ge and Si nanowires, and these values agree reasonably well with the fundamental energy band-gaps of bulk Ge and Si crystals of 0.65 and 1.12 eV. The optical band-edge in  $\text{Si}_{1-x}\text{Ge}_x$  nanowires systematically shifts from that of Si nanowires to that of Ge nanowires with increasing Ge content, and this strongly suggests that the appropriate alloying of our  $\text{Si}_{1-x}\text{Ge}_x$  nanowires gives rise to the energy band-gap modulation. The corresponding variation of optical band-edges is summarized in the inset along with the values measured on bulk crystals from literature.<sup>22</sup> This captures the main focus of this study that the appropriate band-gap modulation of  $\text{Si}_{1-x}\text{Ge}_x$  nanowires between Ge and Si nanowires has been achieved. It is, however, notable that the determined energy band-gaps in  $\text{Si}_{1-x}\text{Ge}_x$  nanowires are lower than those of bulk  $\text{Si}_{1-x}\text{Ge}_x$  crystals, particularly in Ge-rich nanowires, and the onsets of absorption intensity at the threshold energy occur in multiple steps, accompanied by multiple kinks in absorbance. We speculate that one possible reason for this discrepancy between nanowires and bulk crystals is due to the finite variation in composition arising from the statistical distribution of nanowire diameter in the samples.

It should be noted that exciton-Bohr radii, which are primarily responsible for interband optical transitions in semiconductors, are known to be 4.7 and 17.7 nm for Si and Ge crystals.<sup>23</sup> Hence, one can expect to observe quantum size-effects when the diameters of nanowires are close to these characteristic length scales. Indeed, we have observed such size effects on optical absorption from thinner Si and Ge nanowires as shown in Figure 4b. As the mean diameter decreases to 12 and 9 nm for Ge and Si nanowires, the observed band edges of Ge and Si nanowires shift to higher energies up to 1.05 and 2.25 eV; see also the Supporting Information. Here we comment that the effective diameters of nanowires are even smaller than the apparent diameters indicated in Figure 4b, due to the existence of significant oxide shells formed after the growth, as seen in the insets. We also observed a similar blue shift with decreasing diameters in  $\text{Si}_{1-x}\text{Ge}_x$  nanowires by less-pronounced amounts

than those of Si nanowires. Size-dependent light emission in group-IV semiconductors has been extensively investigated particularly for Si nanocrystals, and several mechanisms have been proposed to explain photoluminescence in the visible and ultraviolet ranges.<sup>24,25</sup> These include the excitonic recombination of e–h pairs within Si nanocrystals with the ultraviolet radiation energy, namely, quantum confinement, and the trapped e–h pairs in the Si–O double bonds at the Si surfaces with the characteristic energy of 2.1 eV. It is beyond the scope of this study to discuss an exact origin responsible for our observation of the size-dependent blue shift of optical absorption edges of the thinnest Si and Ge nanowires. It requires further investigation to clarify the issues, such as the control of surface states of thinner nanowires and the photoluminescence lifetime measurements. At the moment, we only comment for qualitative comparison that the 2.25 eV photoluminescence peak is attributed to quantum confinement effect from Si nanocrystals of 3 nm in diameter embedded in  $\text{SiN}_x$  matrices.<sup>26</sup>

In summary, we have successfully synthesized  $\text{Si}_{1-x}\text{Ge}_x$  ( $0 \leq x \leq 1$ ) nanowires and provide evidence of a continuously variable system with crystal lattices and energy band-gaps between Si and Ge nanowires by XRD and optical absorption. In particular, we have tuned the optical band-edge from 0.68 to 2.25 eV by varying both the relative composition of Si and Ge, and the diameter of nanowires, which represent *intrinsic* alloying effects and *extrinsic* size effects, respectively. We argue that our observations can provide interesting implications of Si optoelectronics and Si photonics at the nanometer scale, exploiting energy band-gap modulation in a wide energy range that was not accessible from conventional Si photonics.

**Acknowledgment.** We thank Jae-Beom Shin, Yosep Yang, and Prof. Chan-Gyung Park for TEM observations and Dong-Hwan Yoon and Prof. Sung-Jee Kim for optical absorption measurements and helpful discussions. This work was financially supported by the Korean Research Foundation Grant from the Korean Government (KRF-2005-005-J13103), the Basic Research Program of the Korea Science & Engineering Foundation (R01-2005-000-10711-0), the National Nano Program for Applications (KOSEF 2006-04921), and the Ministry of Information and Communication, Republic of Korea, under project no. A1100-0501-0073.

**Supporting Information Available:** Size-dependent optical absorption of Ge and Si nanowires. This material is available free of charge via the Internet at <http://pubs.acs.org>.

## References

- (1) Madelung, O. In *Semiconductors: Data Handbook*, 3rd ed.; Springer-Verlag: Berlin, 2004.
- (2) For a recent review, see Paul, D. J. *Semicond. Sci. Technol.* **2004**, *19*, R75.
- (3) (a) Ahlgren, D. C.; Dunn, J. *IBM MicroNews* **2000**, 6, 1. (b) Ouellette, J. *The Industrial Physicist* **2002**, June/July, 22.
- (4) Weber, J.; Alonso, M. I. *Phys. Rev. B* **1989**, *40*, 8.
- (5) Lee, J.; Gutierrez-Aitken, A. L.; Li, S. H.; Bhattacharya, P. K. *IEEE Trans. Electron Devices* **1996**, *43*, 2125.
- (6) Davies, G. *Phys. Rep.* **1989**, *176*, 83.

- (7) Takagi, H.; Ogawa, H.; Yamazaki, Y.; Ishizaki, A.; Nakagiri, T. *Appl. Phys. Lett.* **1990**, *56*, 2379.
- (8) (a) Schuppler, S.; Friedman, S. L.; Marcus, M. A.; Adler, D. L.; Xie, Y.-H.; Ross, F. M.; Harris, T. D.; Brown, W. L.; Chabal, Y. J.; Brus, L. E.; Citrin, P. H. *Phys. Rev. Lett.* **1994**, *72*, 2648. (b) van Buuren, T.; Dinh, L. N.; Chase, L. L.; Siekhaus, W. J.; Terminello, L. J. *Phys. Rev. Lett.* **1998**, *80*, 3803.
- (9) Persall, T. P. *Prog. Quantum Optics* **1994**, *18*, 97.
- (10) Duan, X.; Lieber, C. L. *Adv. Mater.* **1999**, *12*, 298.
- (11) Wu, Y.; Fan, R.; Yang, P. *Nano Lett.* **2002**, *2*, 83.
- (12) Lew, K.-K.; Pan, L.; Dickey, E. C.; Redwing, J. M. *Adv. Mater.* **2003**, *15*, 2073.
- (13) Jin, C. B.; Yang, J. E.; Jo, M. H. *Appl. Phys. Lett.*, **2006**, *88*, 193105.
- (14) Kamins, T. I.; Li, X.; Williams, R. S.; Liu, X. *Nano Lett.* **2004**, *4*, 503.
- (15) Wagner, R. S.; Eliis, W. C. *Appl. Phys. Lett.* **1964**, *4*, 89.
- (16) Morales, A. M.; Lieber, C. L. *Science* **1998**, *279*, 208.
- (17) Wu, Y.; Cui, Y.; Huynh, L.; Barrelet, C. J.; Bell, D. C.; Lieber, C. M. *Nano Lett.* **2004**, *4*, 433.
- (18) (a) Zalm, P. C.; van de Walle, G. F. A.; Gravesteijn, D. J.; van Gorkum, A. A. *Appl. Phys. Lett.* **1989**, *55*, 2520. (b) Jesson, D. E.; Pennycook, S. J.; Baribeau, J.-M. *Phys. Rev. Lett.* **1991**, *66*, 750.
- (19) Dismukes, J. P.; Ekstrom, L.; Steigmeier, E. F.; Kudman, I.; Beers, D. S. *J. Appl. Phys.* **1964**, *35*, 2899.
- (20) Dash, W. C.; Newman, R. *Phys. Rev.* **1955**, *99*, 1151.
- (21) Braunstein, R.; Moore, A. R.; Herman, F. *Phys. Rev.* **1958**, *109*, 695.
- (22) Braunstein, R.; Moore, A. R.; Herman, F. *Phys. Rev.* **1958**, *109*, 695.
- (23) Madelung, O. In *Semiconductors: Data Handbook*, 3rd ed.; Springer-Verlag: Berlin, 2004.
- (24) Wolkin, M. V.; Jorne, J.; Fauchet, P. M.; Allan, G.; Delerue, C. *Phys. Rev. Lett.* **1999**, *82*, 197.
- (25) Puzder, A.; Williamson, A. J.; Grossman, J. C.; Galli, G. *Phys. Rev. Lett.* **2002**, *88*, 097401.
- (26) Kim, T. Y.; Park, N. M.; Kim, K. H.; Sung, G. Y.; Ok, Y. W.; Seong, T. Y.; Choi, C. J. *Appl. Phys. Lett.* **2004**, *85*, 5355.

NL0614821